

# Functional applications of stable tau oligomers in cell biology and electrophysiology studies

Emily Hill<sup>1,2</sup>, Kevin G. Moffat<sup>1</sup>, Mark J. Wall<sup>1</sup>, Henrik Zetterberg<sup>3,4,5,6</sup>, Kaj Blennow<sup>3,4</sup>, Thomas K. Karikari<sup>3,7\*</sup>

<sup>1</sup>School of Life Sciences, University of Warwick, Coventry CV4 7AL, UK

<sup>2</sup>Midlands Integrative Biosciences Training Partnership, University of Warwick, Coventry CV4 7AL, UK

<sup>3</sup>Department of Psychiatry and Neurochemistry, Institute of Neuroscience and Physiology, The Sahlgrenska Academy, University of Gothenburg, Sweden

<sup>4</sup>Clinical Neurochemistry Laboratory, Sahlgrenska University Hospital, Mölndal, Sweden

<sup>5</sup>Department of Neurodegenerative Disease, UCL Institute of Neurology, London, UK

<sup>6</sup>UK Dementia Research Institute at UCL, London, UK

<sup>7</sup>Department of Psychiatry, University of Pittsburgh, PA, USA

\*Corresponding author: Thomas K. Karikari, PhD. Department of Psychiatry and Neurochemistry, Institute of Neuroscience and Physiology, The Sahlgrenska Academy, University of Gothenburg, Sweden. Email. [Thomas.Karikari@gu.se](mailto:Thomas.Karikari@gu.se)

Running Head: Cytotoxicity of Tau Oligomers

## Abstract

Aggregated tau protein plays a key role in the pathogenesis of neurodegenerative tauopathies including Alzheimer's disease. Soluble, low molecular weight tau oligomers are formed early in disease processes and are thought to have toxic functions that disrupt neuronal function. The dynamic and transient nature of tau oligomers complicate *in vitro* functional studies to explore the mechanistic links between oligomer formation and neurodegeneration. We have previously described a method of producing stable and structurally characterised oligomers that maintain their oligomeric conformation and prevent further aggregation. This method allows for the flexibility of stabilising tau oligomers by specifically labelling cysteine residues with fluorescent or colourless maleimide conjugates. Here, we describe the functional applications of these preformed stable tau oligomers in cell biology and electrophysiological studies. These investigations allow real-time insights into cellular uptake of exogenous tau oligomers and their functional effects in the recipient cells.

**Keywords:** Tau, Oligomer, Electrophysiology, Tauopathies, Alzheimer's disease

## 1. Introduction

The aggregation of tau protein is a pathological hallmark of Alzheimer's disease and other neurodegenerative tauopathies. The deposition of neurofibrillary tangles (NFTs), the largest-known tau aggregates, in specific brain regions is a neuropathological feature used to confirm a tauopathy diagnosis at *post mortem* [1]. In Alzheimer's disease, tau pathology starts at the preclinical phase, several years ahead of detectable clinical signs at which point NFT formation becomes apparent [2, 3], it is thought that the accumulation of oligomers – low molecular weight tau aggregates that form earlier in the aggregation cascade – better correlate with clinical disease profiles [4]. For this reason, blocking tau aggregation therapeutically is a major research and drug development goal [5, 6]. Recently, tau oligomers have been suggested in animal models to have more direct functional involvements in the

neurodegeneration process, independent of NFT formation. For example, the presence of tau oligomers associates with disease-relevant neurotoxic features including memory, synaptic and mitochondrial defects as well as cell death, often in the absence of NFTs [7,8,9,10,11].

Functional characterization of tau oligomers is often hampered by the transient nature of tau aggregation, which makes it difficult to obtain a pure population of oligomers. To address this challenge, we have developed and verified a method of stabilising tau oligomers [12]. This method is based on the principle of labelling cysteine residues in monomeric tau with maleimide derivatives in specific conditions (*see Chapter X*). Labelling with fluorescent maleimide derivative allows real-time monitoring of tau oligomer function and structural changes in several biochemical contexts, including in cell biology and electrophysiology experiments [13, 14]. In this Chapter, we describe experimental procedures for the application of these stabilised oligomers to study how neuroblastoma cells and human-induced pluripotent stem-cell (hiPSC) derived cortical neurons take up stabilised oligomers exogenously added to the cell media, as well as the effects these aggregates induce intracellularly. Furthermore, we describe a single-cell electrophysiological approach that allows the visualisation of fluorescently labelled tau oligomers mislocalising around the neuron after being introduced directly into the cell soma. This method allows effects on neuronal properties as well as synaptic transmission and plasticity to be measured.

## 2. Materials

The experimental procedures described herein are applicable to both full-length tau-441 and the microtubule-binding region, tau-K18 (amino acids 244-372 of full length tau-441). Note that

the terms “tau oligomers” and “labelled oTau”, anywhere in this chapter, refer to those maleimide-stabilized oligomers of the cysteine-modified K18. All chemicals were obtained from Sigma Aldrich, unless otherwise stated.

## 2.1 Cellular internalisation of tau K18 oligomers

### 2.1.1 SH-SY5Y cells

1. SH-SY5Y cells
2. 1:1 ratio of minimal essential medium (MEM) and F12 Ham medium: 1 % L-Glutamine, 15 % foetal bovine serum, and 1% antibiotic antimycotic acid (10,000 units penicillin, 10 mg streptomycin and 25 µg amphotericin B).
3. CellView™ Advanced Tissue Culture dishes Greiner Bio-One)
4. Alexa Fluor-488-maleimide-labelled tau K18 oligomers i.e., oligomers of the single-cysteine tau construct K18(C291A/C322A/I260C). See **Chapter X** and **[12]** for preparation procedure.
5. Dilute the tau oligomers in the 1:1 MEM/F12 medium to 5 µM. Calculations are based on monomer equivalent
6. Water bath at 37 °C
7. Cell-culture grade incubator set at 37 °C, 5 % CO<sub>2</sub>
8. 1L of 1X phosphate buffered saline (PBS): mix 8 g NaCl, 0.2 g KCl, 1.44 g Na<sub>2</sub>HPO<sub>4</sub>, 0.24 g KH<sub>2</sub>PO<sub>4</sub>. Adjust pH to 7.4.
9. CellMask Deep Red (#C10046, ThermoFisher)
10. FM4-64 dye (N-(3-Triethylammoniumpropyl)-4-(6-(4-(Diethylamino) Phenyl) Hexatrienyl) Pyridinium Dibromide; ThermoFisher)
11. Hoechst 33342
12. LSM 710 microscope (Leica) equipped with an C-Apochromat 63x/1.20 W Korr M27 objective lens
13. ImageJ software (<https://imagej.nih.gov/ij/>)
14. Alexa Fluor-647-labeled anti-human nucleolin antibody

### 2.1.2 Human induced pluripotent stem cell (hiPSC)-derived neurons

1. Neural precursor cells from cord blood CD34 + cells of a healthy, newborn female donor (#ax0016, Axol Bioscience)
2. Tissue culture grade 12-well plates (Corning)
3. 250 µl/cm<sup>2</sup> ReadySet reagent (Axol Bioscience)
4. Cell-culture grade incubator set at at 37 °C, 5 % CO<sub>2</sub>
5. Double distilled water (ddH<sub>2</sub>O).
6. Surebond reagent (#ax0041, Axol Bioscience)
7. Dulbecco's PBS (DPBS)
8. Plasma-cleaned 13 mm glass coverslips
9. Axol Neural Maintenance Medium kit (#ax0031, Axol Bioscience)
10. EVOS XL Core Imaging System (Life Technologies)
11. Stable tau oligomers. See Chapter X and [12] for preparation procedure.
12. 4% paraformaldehyde
13. Permeabilizing solution: DPBS containing 0.2 % Triton.
14. Primary antibody: total tau #A0024 from Agilent (formerly from Dako) or T22, Merck)
15. Secondary antibody: anti-rabbit immunoglobulin G: ThermoFisher #31450
16. Blocking buffer: DPBS, 0.2 % Triton, 2 % BSA.
17. Blocking buffer containing primary antibody and Hoechst.
18. Blocking buffer containing secondary
19. ProLong Gold Antifade mounting medium (#P36934, ThermoFisher Scientific).
20. Leica STP 6000 confocal microscope, 63x objective
21. ImageJ software, <https://imagej.nih.gov/ij>

## 2.2 Impact on neuronal function

### 2.2.1 Slice Preparation

1. Male C57/BL6 mice (2-3 weeks)

2. Microm HM 650V microslicer
3. Cold (2–4°C) high  $Mg^{2+}$ , low  $Ca^{2+}$  aCSF: 127 mM NaCl, 1.9 mM KCl, 8 mM  $MgCl_2$ , 0.5 mM  $CaCl_2$ , 1.2 mM  $KH_2PO_4$ , 26 mM  $NaHCO_3$ , and 10 mM D-glucose pH 7.4
4. Microtome blade
5. Petri dish
6. Filter paper
7. Recording chamber (for slice resting until use)
8. Water bath at 34 °C

### **2.2.2 Recording**

1. Standard artificial cerebrospinal fluid (aCSF): 127 mM NaCl, 1.9 mM KCl, 1 mM  $MgCl_2$ , 2 mM  $CaCl_2$ , 1.2 mM  $KH_2PO_4$ , 26 mM  $NaHCO_3$ , and 10 mM D-glucose
2. Perfusion pump system (2–3 ml/min<sup>-1</sup>)
3. In-bath heating system at 30 °C.
4. Infrared Differential Interference contrast (IR-DIC) optics with an Olympus BX151W microscope (Scientifica)
5. Charged-coupled device (CCD) camera (Hitachi).
6. Patch pipettes (5–10 M $\Omega$ ) manufactured from thick walled glass (Harvard Apparatus).
7. 1 ml syringes
8. Axon multiclamp 700 B amplifier (Molecular Devices) and digitized at 20 kHz.
9. pClamp 10 (Molecular Devices)
10. Tau oligomers, from a 22  $\mu$ M stock (monomer concentration),
11. Filtered intracellular solution: 135 mM potassium gluconate, 7 mM NaCl, 10 mM HEPES, 0.5 mM EGTA, 10 mM phosphocreatine, 2 mM MgATP, and 0.3 mM NaGTP with 293 mOsm and pH 7.2
12. Concentric bipolar electrode (FHC) for LTP/LTD
13. 50  $\mu$ M picrotoxin (to block GABAA receptors)

14. trans-2-carboxy-5,7-dichloro-4-phenylaminocarbonylamino-1,2,3,4-tetrahydroquinoline  
(L689,560; Hello-Bio)

### **2.2.3 Measurements and analysis**

1. Standard IV protocol: step currents from  $-200$  pA incrementing by 50 until a regular firing pattern is induced

The dynamic-I-V curve: defined by the average transmembrane current as a function of voltage during naturalistic activity [15,16,17]; for the dynamic-IV computer code, see [16].

Analysis can be performed using the following software:

1. pClamp/Clampfit software system (version 10.4.2; Molecular devices/ Axon Instruments, CA, USA)
2. MATLAB [18]
3. Julia [19]
4. Prism 6 (GraphPad Inc., CA, USA)

### **2.2.4 Immunohistochemistry and tau localisation**

1. Alexa Fluor 594 hydrazide dye (Invitrogen/ Thermofisher #10072752)
2. Intracellular solution with tau added to a 0.05 mM final concentration
3. Paraformaldehyde (PFA; 4%)
4. PBS
5. Vectashield (Vector Labs).
6. Microscope slides
7. Coverslips
8. Nail varnish
9. Filter paper
10. Leica 880 confocal microscope with Airyscan module

## 3. Methods

### 3.1 Cellular uptake of tau oligomers

#### 3.1.1 SH-SY5Y cell culture

1. Maintain SH-SY5Y cells on 1:1 ratio of minimal essential medium and F12 Ham medium
2. Use cells between passages two and ten for all experiments.
3. Seed the cells at 200,000 cells/ml in CellView Advanced Tissue Culture dishes in the presence of Alexa Fluor-maleimide-labelled tau oligomers dissolved in the culture medium to 5  $\mu$ M.
4. Following 24 h incubation at 37 °C, 5 % CO<sub>2</sub>, remove the spent medium, wash the cells with warm PBS and add fresh tau-free medium containing 2  $\mu$ M Hoechst 33342 and CellMask Deep Red (1:1000 dilution).
5. Perform confocal microscopy imaging of internalized tau after 30 min incubation at 37 °C, 5 % CO<sub>2</sub> using an LSM 710 microscope.
6. Image cells with confocal microscopy without fixing.
7. In internalization analysis, add fresh media containing FM4-64 (2  $\mu$ M) and Hoechst after the PBS wash as described above.
8. Image the cells after 30 min incubation at 37 °C and 5 % CO<sub>2</sub>. Study nucleolin co-localization by adding a 500 X dilution of an Alexa Fluor-647-labeled anti-human nucleolin antibody in tau-free medium to tau oligomer-treated cells after PBS wash
9. Image the cells after 2 h incubation at 37 °C and 5 % CO<sub>2</sub>.
10. Image the cells without fixing, using an LSM 710 (Leica) equipped with an C-Apochromat 63x/1.20 W Korr M27 objective lens.



### 3.1.2 Human induced pluripotent stem cell (hiPSC)-derived neurons

1. Pre-coat tissue culture grade 12-well plates with 250  $\mu\text{l}/\text{cm}^2$  ReadySet reagent, and incubate at 37 °C, 5 %  $\text{CO}_2$  for 45 min and rinse four times with double distilled water.
2. Dilute Surebond reagent in DPBS, and add to the plates at 200  $\mu\text{l}/\text{cm}^2$ . Incubate at 37 °C, 5 %  $\text{CO}_2$  to equilibrate for 1 h.
3. Seed neural precursor cells at a low density (25,000 cells/ $\text{cm}^2$ ) on plasma-cleaned 13 mm glass coverslips, incubate at 37 °C, 5 %  $\text{CO}_2$  and change the media every other day with Axol Neural Maintenance Medium kit for 14–16 days prior to using the cells for experiments.
4. Dilute tau oligomers to 5  $\mu\text{M}$  in Axol Neural Maintenance medium, add to neurons and then incubate for 24 h at 37 °C, 5 %  $\text{CO}_2$ .
5. After removing the spent medium, wash the neurons with DPBS, and add new medium.
6. Fix neurons for 30 min with 4 % paraformaldehyde, wash two times with DPBS, and rinse with permeabilizing solution.
7. Incubate the fixed neurons for 1 h in blocking buffer (DPBS with 0.2 % Triton and 2 % BSA).
8. Incubate for 1 h in the blocking buffer containing primary antibody and Hoechst, at 37 °C and 5 %  $\text{CO}_2$
9. Remove excess antibody by washing thrice with blocking buffer only for 5 min each time.
10. Incubate the neurons in blocking buffer containing secondary antibody for 1 h, and repeat the blocking buffer wash steps.
11. Rinse the slides with distilled water and dip into ProLong Gold Antifade mounting medium
12. Image the neurons with a Leica STP 6000 confocal microscope after at least 24 h of curing. Image the hiPSC-derived cortical neurons with the 63x objective lens, and analyze with the Image J software. Internalization data are expressed as integrated density (area  $\times$  mean fluorescent intensity).

## 3.2 Impact on neuronal function

### 3.2.1 Slice preparation

1. Male BL6 mice (approximately three to four weeks and P12–P21 for paired-synaptic transmission studies) are killed by cervical dislocation and decapitated in accordance with the United Kingdom Animals (Scientific Procedures) Act (1986).
2. Cut parasagittal hippocampal and neocortical slices (350  $\mu\text{M}$ ) with a vibroslicer such as a Microm HM 650V microslicer in cold (2–4 °C) high  $\text{Mg}^{2+}$ , low  $\text{Ca}^{2+}$  aCSF
3. Cut neocortical slices at an angle of +15°, such that the blade started cutting from the surface (layer 1) of the neocortex toward the caudal border of the neocortex [to ensure the integrity of Layer V pyramidal cell (Layer V PC) dendrites [20].
4. Store slices at 34 °C in standard aCSF in a Gibbs chamber for use between 1 and 8 h post slicing.

### 3.2.2 Recording

1. Add either vehicle or tau oligomers, from a 22  $\mu\text{M}$  stock (monomer concentration) to filtered intracellular solution. Note: Intracellular solution should always be filtered before the addition of tau-protein oligomers.
2. Transfer a slice to the recording chamber. Ensure that the slice is submerged and perfused (2–3 ml/min) with aCSF at 30 °C.
3. Visualize the slices using IR-DIC optics with an Olympus BX151W microscope (Scientifica) and a CCD camera (Hitachi).
4. Identify pyramidal cells by their position in the slice, morphology (from fluorescence imaging) and characteristics of the standard current–voltage relationship (Figure 1B).
5. Make whole-cell current-clamp recordings (Figure 1A) from pyramidal cells in area CA1 of the hippocampus and from thick-tufted Layer V PCs in the somatosensory cortex using patch pipettes (5–10  $\text{M}\Omega$ ) manufactured from thick walled glass (Harvard Apparatus). For detailed methods for how to perform patch clamp recording see [21]. In brief, a high resistance seal is formed between the tip of the recording pipette and the membrane of

the target cell. Additional negative pressure is then applied to the pipette, which ruptures the membrane (termed whole-cell breakthrough). The contents of the patch pipette can then dialyze into the target neuron whilst allowing simultaneous current and voltage measurements from the recorded cell (Figure 1B).

6. Make voltage recordings using an Axon Multiclamp 700 B amplifier and digitized at 20 kHz.
7. Perform data acquisition and analysis using the pClamp 10 software suite
8. Recordings from neurons that had a resting membrane potential of between  $-60$  and  $-75$  mV at whole-cell breakthrough are accepted for analysis.
9. The bridge balance should be monitored throughout the experiments and any recordings where it changes by  $>20\%$  should be discarded.

### 3.2.3 Stimulation protocols

To extract the electrophysiological properties of recorded neurons, both step current and naturalistic, fluctuating currents can be injected. Repeat these measurements at 8-10-min time intervals for the duration of recordings in order to develop a time-course for any changes [13, 17].

1. **Standard IV protocol (Figure 1B):** The standard current–voltage relationship can be constructed by injecting step currents from  $-200$  pA (CA1 pyramidal cells) and  $-600$  to  $-400$  pA (Layer V PCs) incrementing by either 50 or 100 pA until a regular firing pattern is induced. A plot of step current amplitude against the voltage response around the resting potential can be used to measure the input resistance (gradient of the fitted line).
2. **Dynamic I-V protocol (Figure 1 C, D, E):** The dynamic-I-V curve, which is defined by the average transmembrane current as a function of voltage during naturalistic activity can be used to efficiently parameterize neurons. It can also be used to generate reduced neural models that accurately mimic the cellular response. The method has been previously described [15, 16, 17]; for the dynamic-IV computer code, see [16].

Briefly, a current wave form, designed to provoke naturalistic fluctuating voltages, was constructed using the summed numerical output of two Ornstein–Uhlenbeck processes [22] with time constants  $\tau_{\text{fast}} = 3$  ms and  $\tau_{\text{slow}} = 10$  ms. This current wave form, which mimics the stochastic actions of AMPA and GABA<sub>A</sub>-receptor channel activation, is injected into cells and the resulting voltage recorded (a fluctuating, naturalistic trace). The voltage trace can then be used to measure the frequency of action potential firing and to construct a dynamic-I-V curve (Figure 1D) and from this a number of parameters can be extracted including resting membrane potential, time constant, capacitance, spike threshold and spike onset (Figure 1E). Using the parameters extracted from the dynamic IV curve, inputted into a refractory exponential integrate-and-fire (rEIF) model can reliably mimic the experimental data, with a spike prediction of ~70–80 % as shown previously [15]. All analyses of the dynamic-I-V traces can be completed using either MATLAB or Julia software platforms [19].

The firing rate can be measured from voltage traces evoked by injecting a current wave form of the same gain factor across all time point recordings [13]. Action potentials are detected by a manually set threshold and then changes to waveform (e.g. amplitude and half-width; Figure 2C) as well as kinetics (rate of rise and decay; Figure 2D) can be calculated. When conducting patch clamp recording, always remember to monitor the series resistance discard any cell varying by more than 10% over the period of recording.

Neurons can be fully reconstructed using the Airyscan module (tiled z-stacks consisting of ~28 stacks each of 260 z-planes) using a Leica 880 confocal microscope to investigate the distribution of oTau in the axon and dendrites (Figure 2B).

### 3.2.6 Localisation of tau oligomers

1. Alexa Flour 594 hydrazide dye (Invitrogen) is added to the intracellular solution (0.05 mM final concentration) to allow cell visualization.

2. CA1 pyramidal neurons injected with labelled oTau are recorded for a minimum of 20 min to allow the diffusion of tau protein out of the pipette and into the cell.
3. The pipette is then carefully removed from the cell
4. Slices are fixed in paraformaldehyde (PFA; 4 %) overnight at 4 °C
5. Slices are then washed five times for five min in PBS the next morning.
6. Slices are mounted and fixed using Vectashield (Vector Labs).
7. A Leica 710 confocal microscope is used for imaging and Zen software for image processing (Figure 2B).

### **3.2.4 Synaptic transmission**

1. To measure synaptic transmission between connected neighbouring neocortical thick-tufted Layer V PCs, make two to three simultaneous whole-cell current-clamp recordings in somatosensory cortex [Figure 3A; **13, 20, 23**]. Clearly the orientation of the synaptic connections will not be known, so the location of the tau oligomers will be randomly distributed in pre and postsynaptic neurons (unless tau is placed in all cells).
2. Recordings are easier from neurons in slices from P12 to P21 mice because unitary EPSPs have a larger amplitude than unitary EPSPs in slices from older mice and show are known to display marked short-term depression [**20, 24**] which can be helpful to measure the effects of oTau on release probability.
3. To determine whether neurons are synaptically connected, evoke action potentials in each cell (using 5 ms current steps) and look for resulting EPSPs in the other recorded cells. As EPSPs can be small in amplitude (as small as 0.1 mV) several sweeps may need to be averaged to confirm connectivity.

4. Once synaptic connectivity is confirmed, evoke six action potentials in the presynaptic neuron (5 at 20 Hz followed by a single recovery action potential after a 1 s interval) using 5 ms current steps (Figure 3B).
5. Repeat these stimulus trains every 10 s and t for the duration of recordings.
6. The amplitude of overlapping unitary EPSPs (evoked by the train) can be accurately measured using voltage deconvolution and reconvolution [20, 25].
7. This protocol will can be used to study both basal synaptic transmission (1<sup>st</sup> EPSP; Figure 3D) and short-term depression (train of 5 EPSPs; Figure 3E).

### 3.2.5 Synaptic plasticity

1. To measure long term potentiation (a measure of synaptic plasticity; LTP), whole-cell current-clamp recordings are made from a CA1 hippocampal pyramidal cell in the presence of 50  $\mu$ M picrotoxin (to block GABA<sub>A</sub> receptors).
2. Picrotoxin (Sigma) and trans-2-carboxy-5,7-dichloro-4-phenylaminocarbonylamino-1,2,3,4-tetrahydroquinoline (L689,560; Hello-Bio) are made as stock solutions (1–50 mM) and diluted in aCSF on the day of use.
3. Stimulate the Schaffer collateral pathway with a concentric bipolar electrode (FHC) every 20 s. Set the stimulus strength so produces reliable EPSPs of ~ 3 mV which are below the threshold to fire action potentials. Then generate at least a 15 min baseline before inducing LTP.
4. LTP can be induced by  $\theta$ -burst stimulation [TBS; 10 trains of 10 stimuli (100 Hz) separated by 100 ms].
5. The potentiation of EPSP amplitude should be measured for at least 30 minutes post-induction. Similar experiments can be used to investigate the effects of Tau oligomers on long term depression using either a paired stimulus protocol or a chemical inducer (such as DHPG)

## Figure legends

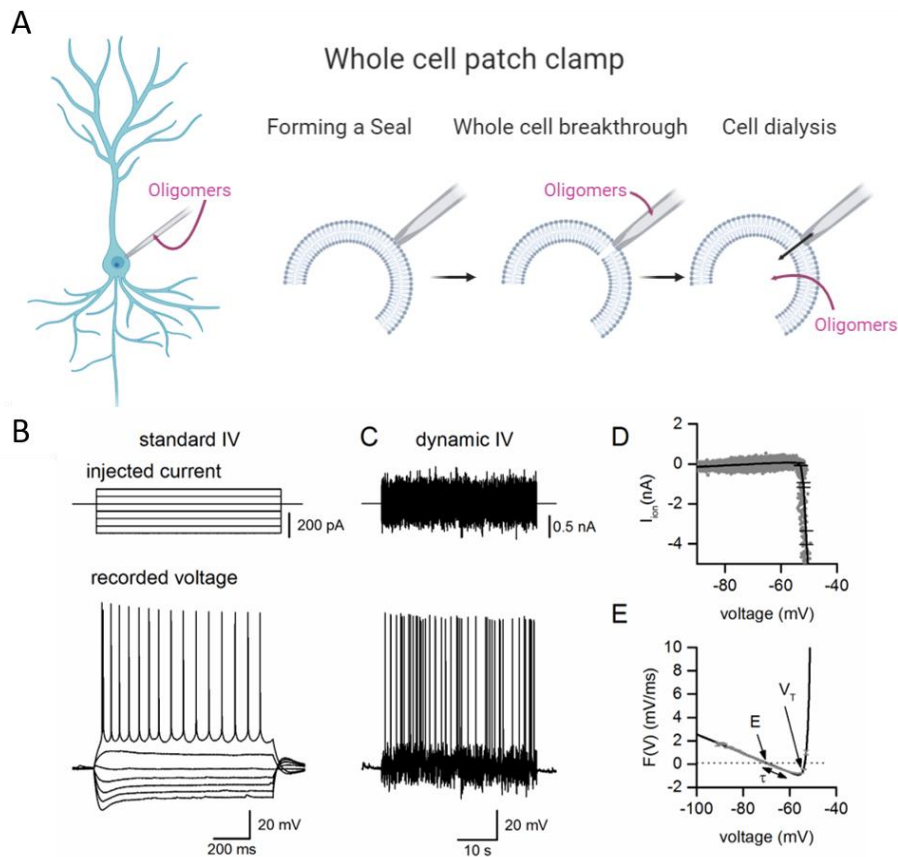


**Figure 1: Whole cell patch clamp and stimulation protocol.** Whole-cell patch clamp recording provides high resolution measurements from single neurons including sub-threshold information (such as changes in membrane potential and input resistance) as well as changes to action potential dynamics. (A) Whole-cell patch clamp protocol, a high resistance seal is formed between the tip of the recording pipette and the membrane of the target cell. Additional negative pressure is then applied to the pipette, which ruptures the membrane (termed whole-cell breakthrough). The contents of the patch-pipette will then dialyse into the cell (delivering the oligomers directly into the soma of the recorded cell). (B) Example of the standard IV protocol used to extract neural parameters: current steps start at -300 pA and are increased by 50 pA (top panel) until a regular firing pattern is induced (bottom panel). Current steps around the resting potential can be used to extract the input resistance. (C) The dynamic IV protocol injects a naturalistic current into the cell (top panel) and the voltage recorded (bottom panel) is used to extract a set of parameters and to determine the firing rate. (D) The mean ionic current  $I_{ion}$  is plotted against membrane potential (grey). The black line is the dynamic IV

curve generated by the average current at a particular voltage (in 1 mV time bins). (E) The negative of  $I_{ion}/C$  is then plotted (grey) along with the EIF (exponential integrate-and-fire) computational model fit, black line. From this curve subthreshold parameters can be extracted (such as resting potential  $E$ , time constant  $\tau$ , spike onset, capacitance and spike-threshold voltage  $V_T$ ). More detail on the method can be found in [15, 16, 17]. *Figure reproduced in part from reference [13] according to an open access CC-BY 4.0 license.*



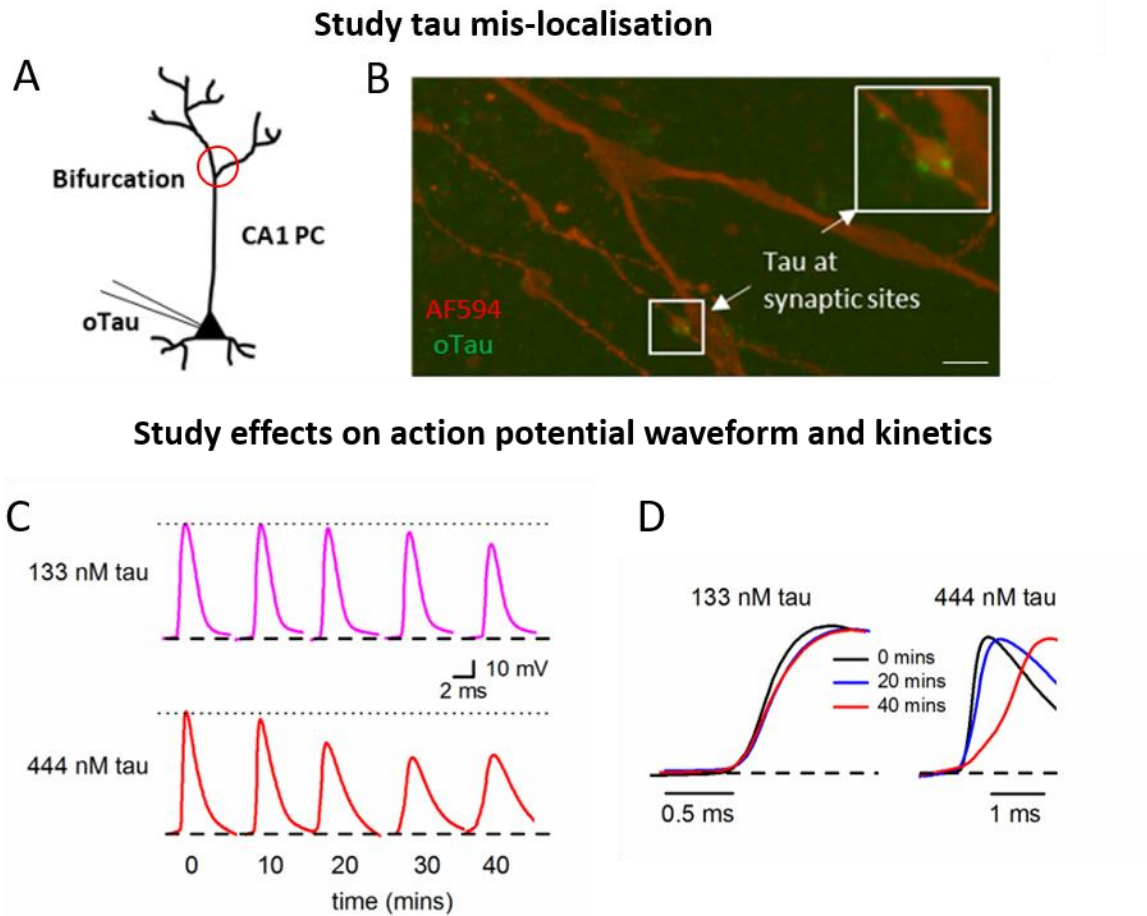


**Figure 2: Tau oligomer localisation and changes to action potential dynamics.** (A) Introducing tau oligomers directly into a single neuron in a network free from pathology permits the study of tau oligomer localisation within the neuron. Labelled tau oligomers are introduced via the pipette (green), along with a different coloured dye (red) and recorded for 30 minutes to allow diffusion within the neuron. (B) The slice is then fixed, and the neuron reconstructed using fluorescence microscopy with the AiryScan Module of the Leica 880 confocal microscope. This allows high resolution imaging of which neuronal compartments (dendrites, axon etc) the tau diffuses into within the recording timeframe. (C) Recording from single cells also permits the study of changes to action potential waveform (e.g. amplitude and half-width) as well as kinetics (rate of rise and decay; (D)). *Figure reproduced in part from reference [13] according to an open access CC-BY 4.0 license.*

### Study direct effects, single neuron resolution

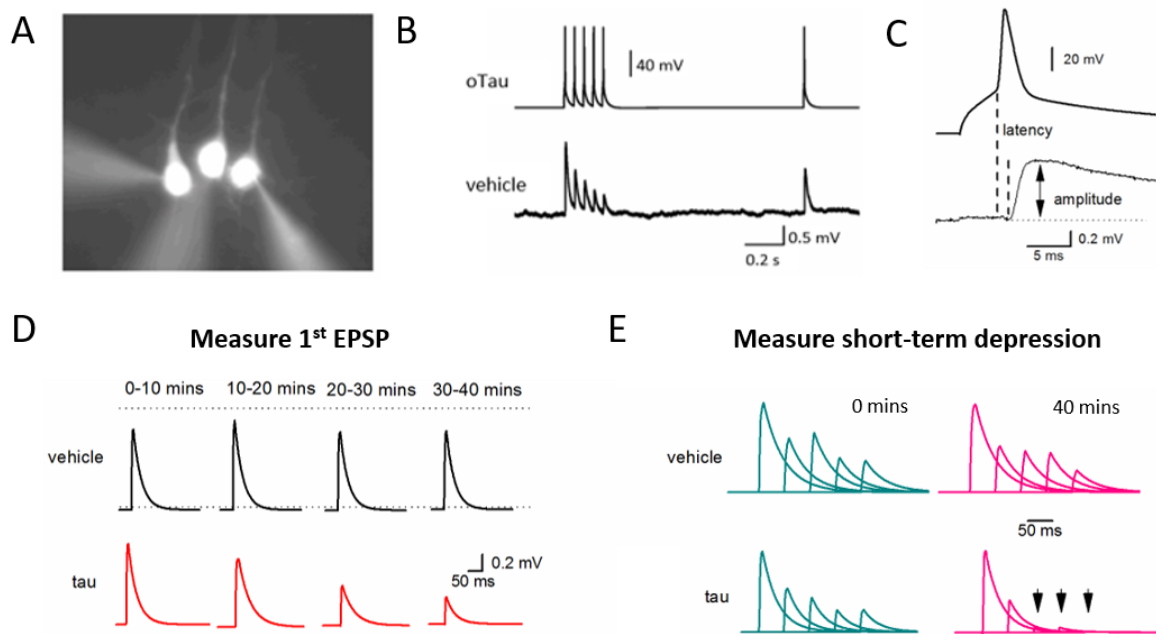


**Figure 3: Studying synaptic transmission.** (A) By making two to three simultaneous whole-cell current-clamp recordings in somatosensory cortex, it is possible to study the effects of tau oligomer introduction on synaptic transmission. Here is an example where 3 layer V pyramidal cells were simultaneously recorded. The neuron on the left has tau oligomers introduced from the patch pipette whereas the other two cells receive vehicle. (B) Start by evoking six action potentials in the presynaptic neuron (5 at 20 Hz followed by a single recovery action potential after a 1 s interval) using 5 ms current steps. (C) This protocol will allow you to measure the amplitude of the evoked excitatory postsynaptic potential (EPSP) in the postsynaptic cell and the latency from the action potential in the presynaptic cell. (D) Comparison of EPSP waveform over time for control vs tau oligomer introduction. (E) Short-term depression can also be evaluated by measuring the EPSP amplitude of each of the 5 EPSPs in the train relative to the 1<sup>st</sup>. You may need to average responses over a number of sweeps if the amplitude is small. Note that the amplitude of overlapping unitary EPSPs (evoked by the train) should be accurately measured using voltage deconvolution and reconvolution [20, 25]. *Figure reproduced in part from reference [13] according to an open access CC-BY 4.0 license.*

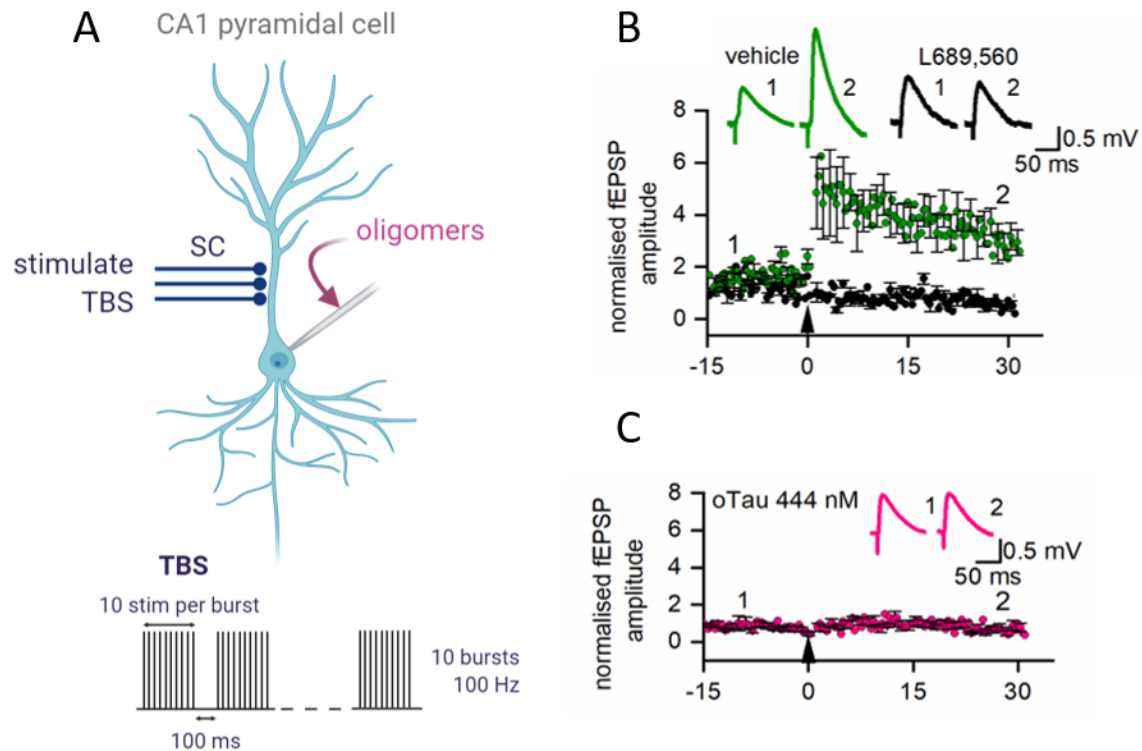


**Figure 4: Studying synaptic transmission.** (A) Diagram of experimental protocol to measure Long term potentiation (LTP). EPSPs are recorded in a single CA1 hippocampal pyramidal cell in response to Schaffer collateral stimulation. LTP is induced by TBS (10 trains of 10 stimuli (100 Hz) separated by 100 ms). (B) Robust LTP can be induced by TBS and is sustained for 30 minutes of recording (green). This can be blocked by the NMDA receptor antagonist L689,560 (black). (C) LTP can then be examined with varying concentrations of tau oligomers within the postsynaptic cell. 444 nM oligomers abolished LTP. *Figure reproduced in part from reference [13] according to an open access CC-BY 4.0 license.*

## Acknowledgements

EH holds a BBRSC-funded PhD studentship. HZ is a Wallenberg Scholar supported by grants from the Swedish Research Council (#2018-02532), the European Research Council (#681712), Swedish State Support for Clinical Research (#ALFGBG-720931), the Alzheimer Drug Discovery Foundation (ADDF), USA (#201809-2016862), the European Union's Horizon 2020 research and innovation programme under the Marie Skłodowska-Curie grant

agreement No 860197 (MIRIADE), and the UK Dementia Research Institute at UCL. KB is supported by the Swedish Research Council (#2017-00915), the Alzheimer Drug Discovery Foundation (ADDF), USA (#RDAPB-201809-2016615), the Swedish Alzheimer Foundation (#AF-742881), Hjärnfonden, Sweden (#FO2017-0243), the Swedish state under the agreement between the Swedish government and the County Councils, the ALF-agreement (#ALFGBG-715986), and European Union Joint Program for Neurodegenerative Disorders (JPND2019-466-236). TKK is a recipient of a Brightfocus Foundation research fellowship (#A2020812F), and is further funded by the Swedish Alzheimer Foundation (Alzheimerfonden; #AF-930627), the Swedish Brain Foundation (Hjärnfonden; #FO2020-0240), the Swedish Dementia Foundation (Demensförbundet), the Agneta Prytz-Folkes and Gösta Folkes Foundation, Gamla Tjänarinnor Foundation, the Aina (Ann) Wallströms and Mary-Ann Sjöbloms Foundation, the Gun and Bertil Stohnes Foundation, and the Anna Lisa and Brother Björnsson's Foundation.

## References

1. H. Braak, E. Braak, Neuropathological staging of Alzheimer-related changes, *Acta Neuropathol.* 82 (1991) 239–259.
2. Karikari, T., Pascoal, T., Ashton, N., et al., 2020. Blood phosphorylated tau 181 as a biomarker for Alzheimer's disease: a diagnostic performance and prediction modelling study using data from four prospective cohorts. *The Lancet Neurology*, 19(5), pp.422-433.
3. R.J. Bateman, C. Xiong, T.L.S. Benzinger, et al., Dominantly Inherited Alzheimer Network, Clinical and biomarker changes in dominantly inherited Alzheimer's disease, *N. Engl. J. Med.* 367 (2012) 795–804,
4. L.L. Beason-Held, J.O. Goh, Y. An, et al., Changes in brain function occur years before the onset of cognitive impairment, *J. Neurosci.* 33 (2013) 18008–18014, <https://doi.org/10.1523/JNEUROSCI.1402-13.2013>.

5. Soeda Y, Yoshikawa M, Almeida OFX, et al., Toxic tau oligomer formation blocked by capping of cysteine residues with 1,2-dihydroxybenzene groups. *Nat Commun.* 2015;6:10216.
6. Yoshitake J, Soeda Y, Ida T, et al. Modification of Tau by 8-nitro-cGMP: Effects of Nitric Oxide-linked Chemical Modification on Tau Aggregation. *J Biol Chem.* 2016;jbc.M116.734350.
7. C. Andorfer, C.M. Acker, Y. Kress, et al. Davies, Cell-cycle re-entry and cell death in transgenic mice expressing nonmutant human tau isoforms, *J. Neurosci.* 25 (2005) 5446–5454, <https://doi.org/10.1523/JNEUROSCI.4637-04.2005>.
8. M. Polydoro, C.M. Acker, K. Duff, et al. Age-dependent impairment of cognitive and synaptic function in the htau mouse model of tau pathology, *J. Neurosci.* 29 (2009) 10741–10749, <https://doi.org/10.1523/JNEUROSCI.1065-09.2009>.
9. C.A. Lasagna-Reeves, D.L. Castillo-Carranza, U. Sengupta, et al., Alzheimer brain-derived tau oligomers propagate pathology from endogenous tau, *Sci. Rep.* 2 (2012), <https://doi.org/10.1038/srep00700>.
10. C.A. Lasagna-Reeves, D.L. Castillo-Carranza, U. Sengupta, et al., Tau oligomers impair memory and induce synaptic and mitochondrial dysfunction in wild-type mice, *Mol. Neurodegener.* 6 (2011) 39, <https://doi.org/10.1186/1750-1326-6-39>.
11. C.A. Lasagna-Reeves, D.L. Castillo-Carranza, U. Sengupta, et al., Identification of oligomers at early stages of tau aggregation in Alzheimer's disease, *Faseb. J.* 26 (2012) 1946–1959, <https://doi.org/10.1096/fj.11-199851>.
12. Karikari TK, Nagel DA, Grainger A, et al. (2019) Preparation of stable tau oligomers for cellular and biochemical studies. *Anal Biochem* 566:67–74.
13. Hill E, Karikari T K, Moffat K G, et al. (2019) Introduction of tau oligomers into cortical neurons alters action potential dynamics and disrupts synaptic transmission and plasticity. *eNeuro* 6 (5) ENEURO.0166-19.2019.

14. Karikari, T., Nagel, D., Grainger, A., et al., (2019). Distinct Conformations, Aggregation and Cellular Internalization of Different Tau Strains. *Frontiers in Cellular Neuroscience*, 13.
15. Badel, L., Lefort, S., Brette, R., et al. 2008a. Dynamic I-V Curves Are Reliable Predictors of Naturalistic Pyramidal-Neuron Voltage Traces. *Journal of Neurophysiology*, 99(2), pp.656-666.
16. Harrison PM, Badel L, Wall MJ et al. (2015) Experimentally verified parameter sets for modelling heterogeneous neocortical pyramidal-cell populations *PLOS Computational Biology* 11: e1004165 (2015)
17. Kaufmann, T., 2015. *The Electrophysiological Impact Of Oligomeric Alpha-Synuclein On Thick-Tufted Layer 5 Pyramidal Neurons In The Neocortex Of Mice*. Ph.D thesis. University of Warwick.
18. MATLAB, 2019b, Natick, Massachusetts: The MathWorks Inc.
19. Bezanson J, Edelman A, Karpinski S, et al. (2017) Julia: a fresh approach to numerical computing. *SIAM Rev* **59**:65–98.
20. Kerr M, Wall M, Richardson M (2013) Adenosine A1 receptor activation mediates the developmental shift at layer 5 pyramidal cell synapses and is a determinant of mature synaptic strength. *J Physiol* **591**:3371–3380.
21. Van Hook M.J., Thoreson W.B. (2014) Whole-Cell Patch-Clamp Recording. In: Xiong H., Gendelman H.E. (eds) *Current Laboratory Methods in Neuroscience Research*. Springer Protocols Handbooks. Springer, New York, NY
22. Uhlenbeck GE, Ornstein LS (1930) On the theory of the Brownian motion. *Phys Rev* 36:823–841
23. Markram H, Lübke J, Frotscher M, et al. (1997) Physiology and anatomy of synaptic connections between thick tufted pyramidal neurones in the developing neocortex. *J Physiol* **500**:409–440.

24. Reyes A, Sakmann B (1999) Developmental switch in the short term modification of unitary EPSPs evoked in layer 2/3 and layer 5 pyramidal neurons in rat neocortex. *J Neurosci* **19**:3827–3835.
25. Richardson MJE, Silberberg G (2008) Measurement and analysis of postsynaptic potentials using a novel voltage-deconvolution method. *J Neurophysiol* **99**:1020–1031.